IOP PUBLISHING PLASMA PHYSICS AND CONTROLLED FUSION

Plasma Phys. Control. Fusion **51** (2009) 055018 (22pp) doi:10.1088/0741-3335/51/5/055018

# Parametric analysis of the two-fluid tearing instability

**Eduardo Ahedo**[1] **and Jesús J Ramos**

Plasma Science and Fusion Center, Massachusetts Institute of Technology, Cambridge, MA, USA

E-mail: eduardo.ahedo@upm.es

Received 12 November 2008, in final form 9 March 2009
Published 9 April 2009
Online at stacks.iop.org/PPCF/51/055018

**Abstract**

A two-fluid analysis of the current driven tearing instability is presented. It concentrates on the systematic investigation of the physics related to the plasma compressibility and to the contribution of the Hall term to the inductive electric field, for arbitrary values of the ion skin depth and of the magnitude of the magnetic guide field. The plasma compressibility is treated consistently for a wide range of the plasma beta that excludes only the extremely cold limit where the mode growth rate would become sonic or supersonic. Conversely, the effects associated with the finite ion gyroradius and the equilibrium density and temperature gradients are neglected. Seven parametric regions are identified, characterized by the relative strengths of the Hall and beta parameters. Five of them are amenable to asymptotic analyses yielding analytic dispersion relations and one allows a semi-analytic treatment. The singular, multi-layer structure of the tearing mode and the conditions under which the different components of the magnetic field diffuse are shown in detail for each of those parametric regions.

## 1. Introduction

The extension of the classic resistive-MHD tearing mode theory [1] to a two-fluid plasma model incorporates a variety of new physics and has been the subject of numerous studies (see, e.g. the detailed discussion and bibliography in [2]). More recently, there has been a renewed interest in accurate two-fluid analytic results that can be used for verification of the new extended-MHD simulation codes. In this regard, the work of [2] provides a broad and updated analysis of the linear tearing instability based on the so-called Hall-MHD model, which is the simplest extension of single-fluid MHD, accounting for distinct ion and electron flows and bringing in physical effects at the length scales of the ion skin depth and the ion sound

[1] Permanent address: Universidad Politécnica de Madrid, Escuela Técnica Superior de Ingenieros Aeronáuticos, Plaza Cardenal Cisneros, 28040 Madrid, Spain.

  

gyroradius, while still neglecting the diamagnetic effects associated with a finite ion Larmor radius. Despite its rather general scope, the analysis of [2] has some limitations, even within the physical model and the specific instability under consideration. In particular, it considers only the 'large magnetic aspect ratio' or 'strong magnetic guide field' limit, where the equilibrium magnetic field has a large component perpendicular to the reconnection plane, relative to its component on that plane. More notably, the ordering schemes leading to the newly proposed asymptotic dispersion relations become inaccurate as the ion skin depth becomes smaller than the macroscopic equilibrium length scale and fail to recover the classic single-fluid result in the limit of vanishing ion skin depth. The purpose of this work is to put forward a complementary study of the linear two-fluid tearing instability that will be continuously accurate for ion skin depths ranging from zero to the equilibrium length scale and beyond, based on the same Hall-MHD plasma model and a similar one-dimensional slab equilibrium without density or temperature gradients, but with arbitrary magnetic aspect ratio. Unlike [2] that extends the analysis to explore the limits of extremely low or zero beta (where the tearing growth rate becomes supersonic) and very large values of the dimensionless tearing instability index $k^{-1}\Delta'$, we will restrict ourselves to consideration of $k^{-1}\Delta' \lesssim 1$ and to at least a minimal value of beta that guarantees subsonic growth rates. These conditions are well satisfied in most applications of interest to magnetically confined plasmas and, in return for these mild restrictions, we will be able to develop a unified formulation that covers general ion skin depths, arbitrary magnetic aspect ratios and the subsonic beta range of main interest, including the complete account of plasma compressibility.

With our working hypotheses of subsonic growth and $k^{-1}\Delta' \lesssim 1$, we will obtain a scaled growth rate that depends on only two independent combinations of primary input data, as the eigenvalue of a compact, unified Hall-MHD tearing mode system, equations (50), (51), (83), (84), valid for the whole relevant parameter space. The two independent input combinations are appropriately scaled versions of the plasma beta, defined here as $\beta = c_s^2/c_A^2$ where $c_s$ and $c_A$ are the sound and Alfven velocities, respectively, and the Hall parameter $\alpha = kd_i$, where $d_i$ is the ion skin depth and $2\pi/k$ is the mode wavelength along its propagating direction. Three well-known dispersion relations will be recovered in three asymptotic domains of our two-dimensional parameter space: for sufficiently small values of the Hall parameter we will get the single-fluid tearing dispersion relation [1], for sufficiently large values of both beta and the Hall parameter we will get the dispersion relation derived with the so-called 'electron-MHD' model [3, 4] and for sufficiently small beta and large Hall parameter we will get the so-called 'semicollisional' tearing dispersion relation [5–7]. We will also carry out the detailed asymptotic analysis of the three parametric regions that cover the transitions between these three classic limits. For sufficiently high beta and general values of the Hall parameter, we will derive a novel analytic dispersion relation that connects the 'single-fluid' and 'electron-MHD' forms. For sufficiently large values of the Hall parameter and general betas, a case whose large magnetic aspect ratio limit was covered by the analysis of [2], we will find the same analytic dispersion relation that connects the 'electron-MHD' and 'semicollisional' forms, now applicable to arbitrary aspect ratios. As far as we are aware, there are no previous detailed studies of the transitional regime between the 'single-fluid' and 'semicollisional' dispersion relations at sufficiently low beta and our work will provide a new semi-analytic solution for this regime.

The paper is organized as follows. Section 2 presents the Hall-MHD model to be considered, with its slab equilibrium and general first-order linearized equations, and identifies the dimensionless parameters of the problem. Section 3 carries out the multiple spatial scale reduction for small resistivity and derives our basic tearing mode system for the non-ideal inner layer, written in terms of appropriately scaled variables. Section 4 is devoted to the solution

of the inner layer equations in the different asymptotic parameter regimes. For each of these, the small-scale structure of the tearing mode and the conditions under which the different components of the magnetic field diffuse are discussed in detail. Section 5 gives the general dispersion relation and its various limits in the different parametric regions. A summarizing discussion is presented in section 6. The main body of the paper is written based on a massless electron model, although the extension to include the effect of a small but finite electron mass on the linear tearing mode is straightforward. The generalization to a finite electron inertia and the modified asymptotic dispersion relations in the collisionless limit, when the inertial term dominates over the resistive friction force in the electron momentum conservation equation, are dealt with in an appendix.

## 2. The model

The basic plasma description to be adopted in this work is provided by a two-fluid, Hall-MHD model with massless electrons and zero-Larmor-radius ions, closed with polytropic equations of state and with an Ohmic resistive term in the generalized Ohm's law as its sole diffusivity (see e.g. [8]):

$$\frac{\partial \boldsymbol{B}}{\partial t} = -\nabla \times \boldsymbol{E}, \tag{1}$$

$$\nabla \cdot \boldsymbol{B} = 0, \tag{2}$$

$$\mu_0 \boldsymbol{j} = \nabla \times \boldsymbol{B}, \tag{3}$$

$$\frac{\partial \rho}{\partial t} + \nabla \cdot \rho \boldsymbol{v} = 0, \tag{4}$$

$$\rho \frac{D\boldsymbol{v}}{Dt} = \boldsymbol{j} \times \boldsymbol{B} - \nabla p = \frac{1}{\mu_0}(\boldsymbol{B} \cdot \nabla)\boldsymbol{B} - \nabla W, \tag{5}$$

$$\boldsymbol{E} = -\boldsymbol{v} \times \boldsymbol{B} + \eta \boldsymbol{j} + \frac{1}{en}(\boldsymbol{j} \times \boldsymbol{B} - \nabla p_\mathrm{e}) = -\boldsymbol{v} \times \boldsymbol{B} + \eta \boldsymbol{j} + \frac{m_\mathrm{i}}{e}\left(\frac{D\boldsymbol{v}}{Dt} + \frac{\nabla p_\mathrm{i}}{\rho}\right), \tag{6}$$

$$p_s n^{-\Gamma_s} = \text{const} \ (s = \mathrm{i}, \mathrm{e}), \tag{7}$$

where $n$ and $\rho = m_\mathrm{i} n$ are the particle and mass densities respectively, $p = p_\mathrm{i} + p_\mathrm{e}$ and the sum of fluid and magnetic pressures $W = p + B^2/2\mu_0$ will be used preferentially instead of $p$; the resistivity $\eta$ will be taken as a constant and the rest of the symbols are conventional.

As zeroth-order solution we will assume a stationary, force-free equilibrium with constant density and temperatures:

$$\rho_0, p_{\mathrm{s}0} = \text{const}, \qquad \boldsymbol{j}_0 \times \boldsymbol{B}_0 = \boldsymbol{0}, \qquad \boldsymbol{v}_0 = \boldsymbol{0}, \qquad \boldsymbol{E}_0 = \eta \boldsymbol{j}_0 \simeq \boldsymbol{0}, \tag{8}$$

where the last condition holds for times smaller than the resistive diffusion time, assumed to be very long. The constant equilibrium density and temperature assumption should of course be viewed just as a first step idealization, that nevertheless allows to address some important two-fluid issues still outstanding. Consideration of more realistic, non-uniform equilibrium density and temperature profiles with their associated diamagnetic effects exceeds the scope of this paper and will be the subject of future work. A one-dimensional equilibrium slab geometry will also be assumed, with the inhomogeneity along the $x$ direction and the magnetic field of the form $\boldsymbol{B}_0 = B_{0y}(x)\boldsymbol{e}_y + B_{0z}(x)\boldsymbol{e}_z$, so that the force-free condition requires that its magnitude $B_0$ be constant. Specifically, we will consider the sheet pinch profiles:

$$B_{0y}(x) = \epsilon_B B_0 \tanh \frac{x}{L} \qquad \text{and} \qquad B_{0z}(x) = [B_0^2 - B_{0y}^2(x)]^{1/2}. \tag{9}$$

The constant $\epsilon_B$ is a measure of the relative strength of the $B_{0y}$ magnetic component and is taken as much less than unity in the customary 'strong magnetic guide field' approximation [2].

In this work, however, we will consider arbitrary guide fields and will treat $\epsilon_B$ as a parameter of order unity. The components of the electric current density are

$$j_{0z} = \frac{1}{\mu_0}\frac{\mathrm{d}B_{0y}}{\mathrm{d}x} = \frac{\epsilon_B B_0}{\mu_0 L}\left(1 - \tanh^2\frac{x}{L}\right) \qquad \text{and} \qquad j_{0y} = -\frac{1}{\mu_0}\frac{\mathrm{d}B_{0z}}{\mathrm{d}x} = j_{0z}\frac{B_{0y}}{B_{0z}}, \tag{10}$$

thus $L$ characterizes the width of the current sheet.

The first-order equations, obtained by linearizing the basic system (1)–(7) about our zeroth-order equilibrium, are as follows:

$$\frac{\partial \boldsymbol{B}_1}{\partial t} = -\nabla\times\boldsymbol{E}_1, \qquad \nabla\cdot\boldsymbol{B}_1 = 0, \tag{11}$$

$$\mu_0\boldsymbol{j}_1 = \nabla\times\boldsymbol{B}_1, \tag{12}$$

$$\boldsymbol{E}_1 = -\boldsymbol{v}_1\times\boldsymbol{B}_0 + \eta\boldsymbol{j}_1 + \frac{m_\mathrm{i}}{e}\left(\frac{\partial \boldsymbol{v}_1}{\partial t} + \frac{\nabla p_{i1}}{\rho_0}\right), \tag{13}$$

$$\frac{\partial \rho_1}{\partial t} + \rho_0\nabla\cdot\boldsymbol{v}_1 = 0, \tag{14}$$

$$\mu_0\rho_0\frac{\partial \boldsymbol{v}_1}{\partial t} = (\boldsymbol{B}_1\cdot\nabla)\boldsymbol{B}_0 + (\boldsymbol{B}_0\cdot\nabla)\boldsymbol{B}_1 - \mu_0\nabla W_1, \tag{15}$$

$$p_1 = c_\mathrm{s}^2\rho_1 = W_1 - \boldsymbol{B}_0\cdot\boldsymbol{B}_1/\mu_0, \tag{16}$$

where $c_\mathrm{s}^2 = (\Gamma_\mathrm{e}T_{\mathrm{e}0} + \Gamma_\mathrm{i}T_{\mathrm{i}0})/m_\mathrm{i}$ is the square of the sound velocity. Since $\rho_0$ is constant, the first-order ion pressure gradient can be absorbed with a redefinition of the electric field:

$$\boldsymbol{E}_1 - \frac{m_\mathrm{i}}{e\rho_0}\nabla p_{\mathrm{i}1} \to \boldsymbol{E}_1.$$

For our present purposes of studying the linear tearing instability as a singular perturbation problem with small resistivity, the generalization of the above system to allow for a small but finite electron inertia is straightforward and amounts simply to a redefinition of the resistivity $\eta$. The details are given in the appendix.

Normal mode perturbations independent of $z$, with periodic spatial variation along the $y$ direction and growth rate $\gamma$ will be considered,

$$f(x, y, t) - f_0(x) = f_1(x)\exp(\gamma t + \mathrm{i}ky), \tag{17}$$

so that the wavenumber vector satisfies $\boldsymbol{k}\cdot\boldsymbol{B}_0 = 0$ at the singular surface $x = 0$.

Set (11)–(16) consists of 14 scalar equations that can be split into a group of six first-order differential equations for $E_{1y}$, $\boldsymbol{B}_1$, $W_1$, and $v_{1x}$, and a group of eight equations that yield algebraically $E_{1x}$, $E_{1z}$, $\boldsymbol{j}_1$, $v_{1y}$, $v_{1z}$, and $\rho_1$ in terms of the other six scalar variables. Once these eight variables are substituted, the six differential equations are as follows:

$$\mathrm{i}B_{1x}' = kB_{1y}, \tag{18}$$

$$\gamma\mu_0\rho_0E_{1y}' = -(\gamma^2\mu_0\rho_0 + k^2B_{0y}^2 + \eta\gamma\rho_0k^2)B_{1z} - k^2B_{0z}(\mu_0W_1 - B_{0y}B_{1y}) - k\frac{B_{0y}'B_0^2}{B_{0z}^2}\mathrm{i}B_{1x} + k\frac{\mathrm{i}m_\mathrm{i}}{e}\gamma^3\mu_0\rho_0\xi, \tag{19}$$

$$\eta B_{1z}' = \mu_0(B_{0z}\gamma\xi - E_{1y}) - \frac{\mathrm{i}m_\mathrm{i}}{e\rho_0}[B_{0y}'\mathrm{i}B_{1x} + k(\mu_0W_1 - B_{0y}B_{1y})], \tag{20}$$

$$\eta kB_{1y}' = (\mu_0\gamma + \eta k^2)\mathrm{i}B_{1x} + \mu_0kB_{0y}\gamma\xi - \frac{\mathrm{i}m_\mathrm{i}}{e\rho_0}kB_{0y}\left(\frac{B_{0y}'}{B_{0z}}\mathrm{i}B_{1x} + kB_{1z}\right), \tag{21}$$

$$\gamma^2\mu_0\rho_0\xi' = -kB_{0y}'\mathrm{i}B_{1x} - k^2(\mu_0W_1 - B_{0y}B_{1y}) - \gamma^2\mu_0\rho_1, \tag{22}$$

$$\mu_0W_1' = kB_{0y}\mathrm{i}B_{1x} - \gamma^2\mu_0\rho_0\xi, \tag{23}$$

where the prime ($'$) denotes the derivative with respect to $x$; we have introduced the Lagrangian displacement variable

$$\xi = \gamma^{-1} v_{1x}$$

and the perturbed density, satisfying the algebraic relation

$$(c_s^2 k^2 + \gamma^2)\rho_1 = -\gamma^2 \rho_0 \xi' - \frac{k B_{0z}}{\mu_0}\left(k B_{1z} + \frac{B'_{0y}}{B_{0z}} \mathrm{i} B_{1x}\right), \tag{24}$$

is to be substituted in equation (22).

This set of first-order equations can be written, in a more conventional way, as the following set of three second-order differential equations for ($\xi$, $B_{1x}$, $B_{1z}$):

$$\gamma^2 \mu_0 \left(\rho_0 \nabla^2 \xi + \rho_1'\right) = \mathrm{i}k(B_{0y}\nabla^2 B_{1x} - B''_{0y} B_{1x}), \tag{25}$$

$$\eta \nabla^2 B_{1x} = \gamma \mu_0 (B_{1x} - \mathrm{i}k B_{0y}\xi) - \frac{m_\mathrm{i}}{e\rho_0} k B_{0y}\left(k B_{1z} + \frac{B'_{0y}}{B_{0z}} \mathrm{i} B_{1x}\right), \tag{26}$$

$$\eta\gamma\rho_0 \nabla^2 B_{1z} = k B_{0y}^2 \left(k B_{1z} + \frac{B'_{0y}}{B_{0z}} \mathrm{i} B_{1x}\right) - \gamma^2 \mu_0 (B_{0z}\rho_1 - \rho_0 B_{1z})$$
$$- \frac{m_\mathrm{i}}{e}\gamma \left(B_{0y}\nabla^2 B_{1x} - B''_{0y} B_{1x}\right), \tag{27}$$

with $\nabla^2 \equiv \mathrm{d}^2/\mathrm{d}x^2 - k^2$ and the algebraic equation (24) for $\rho_1$. It is worth noting that equations (24)–(27) follow exactly from the general linearized set, equations (11)–(16), wihout any simplifying assumptions. In the limit $\epsilon_B \ll 1$, these equations recover the model considered by Mirnov *et al* [2] except that they use a second-order differential equation for $\rho_1$ instead of our algebraic equation (24).

The linear stability analysis must determine the dimensionless growth rate

$$\epsilon_\gamma = \frac{\gamma}{c_\mathrm{A} k}, \tag{28}$$

in terms of the five independent dimensionless parameters of the problem:

$$\epsilon_\eta = \frac{\eta k}{\mu_0 c_\mathrm{A}}, \qquad \alpha = k d_\mathrm{i}, \qquad \beta = \frac{c_s^2}{c_\mathrm{A}^2}, \qquad \epsilon_B = \frac{B_{0y}(\infty)}{B_0} \qquad \text{and} \qquad kL, \tag{29}$$

where $c_\mathrm{A} = B_0(\mu_0\rho_0)^{-1/2}$ is the Alfven velocity and $d_\mathrm{i} = m_\mathrm{i}(e^2\mu_0\rho_0)^{-1/2}$ is the ion skin depth. The parameter $\epsilon_\eta$ is the inverse of the magnetic Reynolds number $S$ based on the length $k^{-1}$. In addition to the ion skin depth characteristic of the Hall effects, one can define the lengths

$$d_s = d_\mathrm{i}\sqrt{\beta} = m_\mathrm{i} c_s/(eB_0), \qquad d_\eta = \epsilon_\eta/k, \qquad d_\gamma = \epsilon_\gamma/k, \tag{30}$$

associated with compressible, resistive and inertial effects, respectively. Table 1 details typical values of these parameters in some tokamak plasmas. Notice the extremely low value of $\epsilon_\eta$, which will be our fundamental expansion parameter. Resistive effects will matter only within a thin layer around $x = 0$ where $\boldsymbol{k}\cdot\boldsymbol{B}_0 \simeq 0$ [1], leading to the familiar, multiple scale tearing mode analysis for $\epsilon_\eta \to 0$. As mentioned before, the magnetic geometry inverse aspect ratio parameter $\epsilon_B$ will be assumed to be of order unity, thus allowing for arbitrary magnetic guide fields. Our only constraint on the beta parameter will be $\beta \gg \epsilon_\gamma^2$, which is well satisfied in tokamak plasmas and excludes just the extremely cold limit where the tearing mode growth rate would become sonic or supersonic. The Hall parameter $\alpha$ will only be restricted by compatibility with the above subsonic growth condition. This will set an upper limit on $\alpha$

**Table 1.** Typical plasma parameters in two representative tokamaks (A: Alcator C-MOD; I: ITER) with deuterium ions. For reference, the characteristic single-fluid growth rate $\gamma_0 = c_A k \epsilon_\eta^{3/5}$, with $k = 3/r$, is used.

| | A | I |
|---|---|---|
| $r$ (m) | 0.2 | 2 |
| $B_0$ (T) | 5 | 5 |
| $\epsilon_B$ | 0.33 | 0.33 |
| $n_e$ ($10^{20}$ m$^{-3}$) | 2 | 1 |
| $T_e$, $T_i$ (keV) | 1 | 10 |
| $\eta$ ($10^{-8}$ $\Omega$ m) | 4.7 | 0.18 |
| $d_i$ (mm) | 23 | 32 |
| $d_e$ (mm) | 0.38 | 0.53 |
| $\alpha$ ($10^{-2}$) | 34.3 | 4.8 |
| $\beta$ ($10^{-2}$) | 0.54 | 2.7 |
| $\epsilon_\eta$ ($10^{-8}$) | 10 | 0.027 |
| $\alpha\epsilon_\eta^{-1/5}$ | 8.5 | 4.0 |
| $\beta\epsilon_\eta^{-2/5}$ | 3.3 | 180 |
| $\gamma_0$ (s$^{-1}$) | 5200 | 21 |

depending on $\beta$, that will be of the order of $\epsilon_\eta^{-1/5}$ or greater so that the entire practical range from the single-fluid to the strong-Hall regimes will be covered. Finally, $kL$ will be taken as order unity but required to be such that the tearing instability index $k^{-1}\Delta'$ is also of order unity or less: the exclusion of very large values of $k^{-1}\Delta'$, which is sensible for most realistic applications, turns out in fact to be the most restrictive condition in our analysis.

## 3. Multiple spatial scale formulation

The linear tearing mode analysis is based on the classic singular perturbation theory for $\epsilon_\eta \ll 1$ [1], which yields a growth rate scaling as a fractional power of the resistivity, $\epsilon_\gamma \propto \epsilon_\eta^\nu$ ($0 < \nu < 1$), and a mode eigenfunction structure on multiple spatial scales, resistive effects being important only within a microscopic region near $x = 0$ where $\boldsymbol{k} \cdot \boldsymbol{B}_0 \simeq 0$.

In the outer region where $kx$ and $x/L$ are considered to be of order unity, one can take the dissipationless and quasi-stationary limits, $\epsilon_\eta \to 0$ and $\epsilon_\gamma \to 0$. Then, in their leading orders, equation (25) reduces to

$$B_{0y} B_{1x}'' - (k^2 B_{0y} + B_{0y}'') B_{1x} = 0 \tag{31}$$

and equation (27) reduces to

$$k B_{1z} = -\mathrm{i} \frac{B_{0y}'}{B_{0z}} B_{1x}. \tag{32}$$

Moreover, combining equations (25) and (27) and anticipating the scaling $\epsilon_\gamma \propto \epsilon_\eta^\nu \gg \epsilon_\eta$, one finds that $k B_{1z} + \mathrm{i} B_{0y}' B_{0z}/B_{1x}$ will scale proportional to $\epsilon_\gamma^2$, hence the leading order of equation (26) yields

$$k\xi = -\mathrm{i} B_{1x}/B_{0y} \tag{33}$$

and the leading order of equation (24) yields

$$\rho_1 = 0. \tag{34}$$

Therefore, this outer region system, equations (31)–(34), is identical to the one obtained in ideal-MHD but is valid for any value of $\alpha$ and, like ideal-MHD at marginal stability, is incompressible for any value of $\beta$.

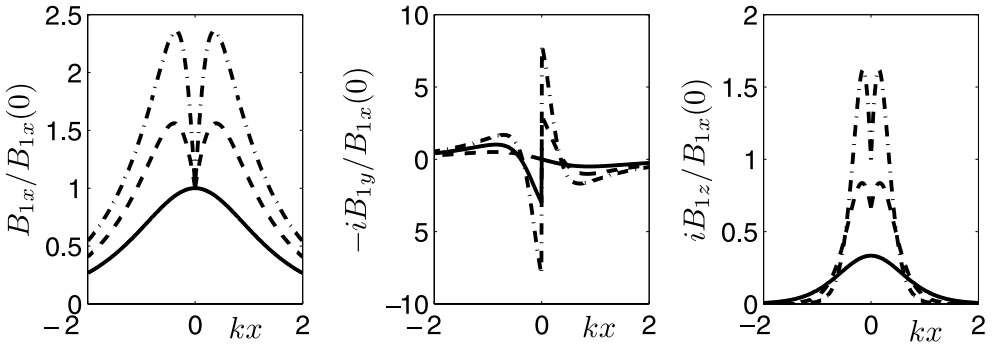


**Figure 1.** Components of the perturbed magnetic field $\boldsymbol{B}_1(x)$, for $\epsilon_B = 1/3$ and sheet pinch profiles with $kL = 1$ (solid), 1/2 (dashed) and 1/3 (dash-and-dot) (yielding $\Delta' \simeq 0$, 4 and 13, respectively).

For the sheet pinch equilibrium profile of equation (9), the solution to equation (31) satisfying the boundary conditions $B_{1x}(\pm\infty) = 0$ is

$$B_{1x}(x) = B_{1x}(0)\mathrm{e}^{-k|x|}\left(1 + \frac{1}{kL}\tanh\frac{|x|}{L}\right) \tag{35}$$

and figure 1 illustrates the corresponding three components of the perturbed magnetic field. There is a discontinuity in $B'_{1x} = -\mathrm{i}kB_{1y}$ and $B'_{1z}$ at $x = 0$,

$$\frac{B'_{1x}\big|_{x=0^-}^{x=0^+}}{kB_{1x}(0)} = \frac{-\mathrm{i}B_{1y}\big|_{x=0^-}^{x=0^+}}{B_{1x}(0)} = \frac{B'_{1z}\big|_{x=0^-}^{x=0^+}}{kB_{1z}(0)} \equiv k^{-1}\Delta' \tag{36}$$

with

$$k^{-1}\Delta' = 2[(kL)^{-2} - 1]. \tag{37}$$

The condition for tearing mode instability is $\Delta' > 0$ [1], corresponding to the range $kL < 1$. Notice that, for finite magnetic aspect ratios, the component $B_{1z}$ is comparable to $B_{1x}$ and should not be neglected: $B_{1z}(0)/B_{1x}(0) = \epsilon_B/(kL)$.

For $x \ll L$, one has

$$B_{0y} \simeq \epsilon_B B_0 x/L \qquad \text{and} \qquad B_{0z} \simeq B_0 \tag{38}$$

so that equation (33) implies that $\mathrm{i}k\xi \propto L/x \to \infty$ for $x/L \to 0$. A boundary layer must develop around $x = 0$ in order to bound $k\xi$ and smooth the discontinuities in the components of the perturbed magnetic field, matching regularly the $x < 0$ and $x > 0$ branches of the outer solution. This boundary layer, where non-ideal effects neglected in the outer region must be taken into account, must have a width much smaller than the equilibrium current sheet width, $L$, and may include several distinct asymptotic sublayers depending on the plasma parameters. Within it, equilibrium quantities can be approximated by the leading terms of their Taylor expansions about $x = 0$, equation (38), and the length scales associated with the gradients of perturbed quantities along $x$ are much shorter than $L$. In particular, the Laplacian operator acting on perturbed quantities can be approximated as $\nabla^2 \simeq \mathrm{d}^2/\mathrm{d}x^2$. The only exception is $B_{1x}$ (whose outer solution is continuous) that varies on the scale of $L$, although its discontinuous first derivative $\mathrm{d}B_{1x}/\mathrm{d}x = -\mathrm{i}kB_{1y}$ varies on the short scales of the boundary layer. Accordingly, we will adopt the 'constant-$B_{1x}$ approximation' whereby $B_{1x}$ is replaced by the constant $B_{1x}(0)$ through the non-ideal layer, while its derivative is still treated as an $x$-dependent dynamical variable. The $B_{1z}$ component has a continuous outer solution, equation (32), and might therefore have been expected to exhibit the same slower variation as

$B_{1x}$. This is indeed the case in single-fluid resistive-MHD, but the two-fluid Hall effects give rise to an additional, fast-varying and internally localized, contribution to $B_{1z}$ with the opposite (odd) parity. This two-fluid, odd part of $B_{1z}$ is conveniently represented by the variable

$$Q = B_{1z} + \mathrm{i} B_{1x} B'_{0y}/(k B_{0z}), \tag{39}$$

such that the residual $B_{1z} - Q$ is the even parity extension into the boundary layer of the functional form of the outer solution, linked to $B_{1x}$. Using the above discussed simplifications based only on the application to a short-scale boundary layer around $x = 0$, introducing the equilibrium magnetic gradient scale length $L_B \equiv L/\epsilon_B$, and in terms of $Q$ as primary variable instead of $B_{1z}$, our basic linear system equations (24)–(27) becomes

$$(\beta + \epsilon_\gamma^2)\frac{\rho_1}{\rho_0} = -\epsilon_\gamma^2 \xi' - \frac{Q}{B_0}, \tag{40}$$

$$\epsilon_\eta \frac{B''_{1x}}{k^2 B_0} = \epsilon_\gamma \left( \frac{B_{1x}(0)}{B_0} - \frac{x}{L_B} k \mathrm{i} \xi \right) - \alpha \frac{x}{L_B}\frac{Q}{B_0}, \tag{41}$$

$$\frac{\epsilon_\gamma^2 \beta}{\beta + \epsilon_\gamma^2} \mathrm{i}\xi'' + \frac{x}{L_B}\frac{B''_{1x}}{k B_0} = \mathrm{i}\frac{\epsilon_\gamma^2}{\beta + \epsilon_\gamma^2}\frac{Q'}{B_0}, \tag{42}$$

$$\epsilon_\eta \epsilon_\gamma \frac{Q''}{k^2 B_0} - \left( \frac{x^2}{L_B^2} + \epsilon_\gamma^2 \frac{1 + \beta + \epsilon_\gamma^2}{\beta + \epsilon_\gamma^2} \right) \frac{Q}{B_0} + \epsilon_\gamma \alpha \frac{x}{L_B}\frac{B''_{1x}}{k^2 B_0}$$

$$= -\mathrm{i}\epsilon_\gamma \frac{x}{k L_B^2} \left( \epsilon_\gamma k \mathrm{i}\xi + \alpha \frac{Q}{B_0} \right) - \mathrm{i}\frac{\epsilon_\gamma^4 \mathrm{i}\xi'}{\beta + \epsilon_\gamma^2}, \tag{43}$$

where $B''_{1x}$ can be eliminated algebraically by substituting equation (41) into equations (42) and (43). Thus, the explicit calculations of $\rho_1$ and $B'_{1x}$ become decoupled from the pair of equations that determine $\xi$ and $Q$, and can be carried out *a posteriori* once the latter have been solved for.

Equations (40)–(43) represent the most general inner system that follows from the original linear set, (11)–(16), under the sole assumption of a short-scale layer around $x = 0$ for $\epsilon_\eta \ll 1$. This system will be further reduced by implementing the following orderings that constitute our main working hypotheses:

$$\epsilon_B = O(1), \qquad k^{-1}\Delta' = O(1), \qquad \beta \gg O(\epsilon_\gamma^2). \tag{44}$$

As mentioned earlier, these orderings allow arbitrary magnitudes of the magnetic guide field and all practical values of the Hall parameter, and exclude only extremely low betas and very large values of $k^{-1}\Delta'$. Condition (44) on $\beta$ limits our analysis to subsonic tearing mode growths, $\gamma \ll k c_s$, which is largely the sole case of practical interest. Sonic or supersonic growths would only be approached in the excluded regimes of extremely low $\beta$ or very large $k^{-1}\Delta'$, which are not relevant to most realistic applications. The solutions to be obtained will also confirm that these conditions allow the consistent neglect of the right-hand sides of equations (42) and (43). With these simplifications, these equations become

$$\frac{\epsilon_\gamma \epsilon_\eta}{k} \mathrm{i}\xi'' = \frac{x}{L_B} \left( -\frac{B_{1x}(0)}{B_0} + \frac{x}{L_B} k \mathrm{i}\xi + \frac{\alpha}{\epsilon_\gamma}\frac{x}{L_B}\frac{Q}{B_0} \right), \tag{45}$$

$$\epsilon_\eta \epsilon_\gamma \frac{Q''}{k^2 B_0} = \left( \frac{x^2}{L_B^2} + \epsilon_\gamma^2 \frac{1 + \beta}{\beta} \right) \frac{Q}{B_0} + \frac{\epsilon_\gamma^3 \alpha}{k} \mathrm{i}\xi''. \tag{46}$$

Equations (45) and (46) yield real solutions for $\mathrm{i}\xi / B_{1x}(0)$ and $Q/B_{1x}(0)$ and, as a consequence, equations (36) and (41) yield a real $\epsilon_\gamma$. The right-hand sides of equations (42) and (43) would

make $i\xi/B_{1x}(0)$ or $Q/B_{1x}(0)$ complex, resulting in a complex growth rate. Thus, our working hypotheses (44) ensure also that, in their domain of validity, the tearing mode is purely growing.

The last step is to write the inner system (45) and (46) in dimensionless form. To this effect we introduce the characteristic length $d_0$ defined by

$$d_0 = L_B^{1/2}(d_\eta d_\gamma)^{1/4} = (\epsilon_\gamma \epsilon_\eta)^{1/4}(L_B/k)^{1/2}, \tag{47}$$

the dimensionless variables

$$\bar{x} = \frac{x}{d_0}, \qquad \bar{\xi} = \frac{d_0 B_0}{L_B B_{1x}(0)} ki\xi, \qquad \bar{Q} = \frac{d_0 \alpha}{L_B \epsilon_\gamma} \frac{Q}{B_{1x}(0)}, \tag{48}$$

and the dimensionless parameters

$$\sigma = \alpha \epsilon_\gamma^{1/2} \epsilon_\eta^{-1/2}, \qquad \tau = (\beta^{-1} + 1)\epsilon_\gamma^{3/2} \epsilon_\eta^{-1/2} k L_B. \tag{49}$$

In terms of these, equations (45) and (46) become

$$\frac{\mathrm{d}^2\bar{\xi}}{\mathrm{d}\bar{x}^2} = \bar{x}^2(\bar{\xi} + \bar{Q}) - \bar{x}, \tag{50}$$

$$\frac{\mathrm{d}^2\bar{Q}}{\mathrm{d}\bar{x}^2} = (\bar{x}^2 + \tau)\bar{Q} + \sigma^2 \frac{\mathrm{d}^2\bar{\xi}}{\mathrm{d}\bar{x}^2}, \tag{51}$$

which constitute the fundamental inner tearing mode system for our present two-fluid analysis. Definitions (48) and (49) of dimensionless inner variables and parameters rely on the idea that inertial and resistive effects establish the basic natural scales for the tearing mode system, (50) and (51). There, the terms proportional to $\sigma^2$ and $\tau$ measure the Hall and $\beta$ (i.e compressibility) effects, respectively. The mathematical scaling parameters $\sigma^2$ and $\tau$ involve the yet to be determined $\epsilon_\gamma$, so we have to wait until the mode growth rate has been found to define the relevant two basic input parameters in terms of the primary dimensionless data of equation (29). The solution of equations (50) and (51) yields $\bar{\xi}$ and $\bar{Q}$ as a *real, odd* function of $\bar{x}$, depending parametrically on $\sigma$ and $\tau$. Their boundary conditions are $\bar{\xi} = \bar{Q} = 0$ at $\bar{x} = 0$ and

$$\bar{\xi} = \bar{x}^{-1} + 2(1+\sigma^2)\bar{x}^{-5} + \cdots, \quad \bar{Q} = -2\sigma^2\bar{x}^{-5} + \cdots, \qquad \text{for} \quad \bar{x} \gg \{1, \tau^{1/2}\}. \tag{52}$$

For reference, it is illustrative to examine the dispersion relation for plane waves in a homogeneous plasma that would correspond to our reduced model. This is obtained by making the identifications $kx/L_B \to k_\parallel$, $-\mathrm{d}^2/\mathrm{d}x^2 \to k_\perp^2 \gg k_\parallel^2$ and $\gamma^2 = -\omega^2$ in equations (45) and (46) complemented by equation (41) for $B_{1x}$. The result is an algebraic system that yields (neglecting also the resistivity which only damps the waves here)

$$(\omega^2 - k_\parallel^2 c_\mathrm{A}^2)[\omega^2(1+\beta) - k_\parallel^2 c_\mathrm{s}^2] - \omega^2 k_\perp^2 d_\mathrm{i}^2 k_\parallel^2 c_\mathrm{s}^2 = 0. \tag{53}$$

This dispersion relation represents the shear-Alfven-like (also called kinetic-Alfven) and slow-magnetoacoustic-like branches of Hall-MHD for near-perpendicular propagation, $k_\perp^2 \gg k_\parallel^2$. The fast-magnetoacoustic-like branch that becomes the whistler wave in Hall-MHD has been eliminated by our reduction.

## 4. Inner region solution in different parametric regimes

The inner tearing mode solution depends on the two dimensionless parameters $\sigma$ and $\tau$ defined in equation (49). Seven parametric regions (PR0, PR1, ..., PR6) can be distinguished in a $(\sigma, \tau)$ plane, as sketched in figure 2. There is the parametric region PR0, with $\sigma = O(1)$ and $\tau = O(1)$, where the full equations (50) and (51) have to be solved numerically. In the other six regions, these equations admit some asymptotic reduction. In some of them, the inner boundary layer splits into two asymptotic sublayers: an intermediate, non-resistive layer of characteristic

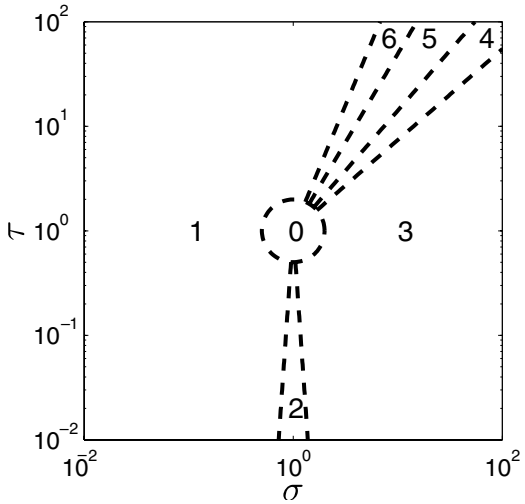


**Figure 2.** Location of the different asymptotic regions in the plane of mathematical scaling parameters.

**Table 2.** Main characteristics of parametric regions PR1 to PR6. A black circle means 'yes'.

| | PR1 | PR2 | PR3 | PR4 | PR5 | PR6 |
|---|---|---|---|---|---|---|
| Mathematical scaling parameters | $\sigma \ll 1$ or $\tau \gg \sigma^2$ | $\sigma \sim 1$ and $\tau \ll 1$ | $\sigma \gg 1$ and $\tau \ll \sigma$ | $\sigma \gg 1$ and $\tau \sim \sigma$ | $\sigma \gg 1$ and $\sigma \ll \tau \ll \sigma^2$ | $\sigma \gg 1$ and $\tau \sim \sigma^2$ |
| $B_x$-diffusion | • | • | • | • | • | • |
| $B_z$-diffusion | | • | • | • | | |
| Hall effects | | • | • | • | • | • |
| Compressibility | | | | • | • | • |
| Two sublayers | | | • | • | • | |
| Dominant field | $\bar{\xi}$ | $\bar{\xi}, \bar{Q}$ | $\bar{Q}$ | $\bar{Q}$ | $\bar{Q}$ | $\bar{\xi}, \bar{Q}$ |
| Primary input parameters | $\hat{\alpha} \ll 1$ or $\hat{\beta} \ll \hat{\alpha}^{-2}$ | $\hat{\alpha} \sim 1$ and $\hat{\beta} \gg 1$ | $\hat{\alpha} \gg 1$ and $\hat{\beta} \gg \hat{\alpha}^{-1/2}$ | $\hat{\alpha} \gg 1$ and $\hat{\beta} \sim \hat{\alpha}^{-1/2}$ | $\hat{\beta} \ll \hat{\alpha}^{-1/2}$ and $\hat{\beta} \gg \hat{\alpha}^{-2}$ | $\hat{\alpha} \gg 1$ and $\hat{\beta} \sim \hat{\alpha}^{-2}$ |

width $d_2$ and an innermost, resistive layer of width $d_1 \ll d_2$. When this is the case, the length $d_0$, equation (47), is the geometric mean of the two sublayer lengths, $d_0 = \sqrt{d_1 d_2}$. Otherwise, these two layers merge into a single one of width $d_0$. The characteristics of the tearing mode solutions in each of these parametric regions are summarized in table 2.

Before proceeding with the specific asymptotic solutions for the different parametric regimes (PR1, ..., PR6), some general features of our tearing mode system, equations (50) and (51), are worth commenting on. First, if we drop all second-order derivatives in equations (50) and (51), we are neglecting all resistive and dynamic effects and recover the asymptotic form of the outer solution, $\bar{Q} = 0$ and $\bar{\xi} = 1/\bar{x}$. Second, dropping the lhs of equations (50) and (51) corresponds to neglecting just the resistivity effects and leads to

$$\frac{\mathrm{d}^2\bar{\xi}}{\mathrm{d}\bar{x}^2} = \frac{(\bar{x}^2+\tau)(\bar{x}^2\bar{\xi}-\bar{x})}{\sigma^2\bar{x}^2} = -\bar{Q}\frac{\bar{x}^2+\tau}{\sigma^2}, \tag{54}$$

which are the equations for the intermediate layer whenever it exists independently of the innermost resistive layer. Third, dropping only the lhs of equation (51) leads to

$$\frac{\mathrm{d}^2\bar{\xi}}{\mathrm{d}\bar{x}^2} = \frac{(\bar{x}^2+\tau)(\bar{x}^2\bar{\xi}-\bar{x})}{(1+\sigma^2)\bar{x}^2+\tau} = -\bar{Q}\frac{\bar{x}^2+\tau}{\sigma^2}, \tag{55}$$

which is the model of the resistive layer when the diffusion of $B_{1z}$ is negligible. Notice that $\mathrm{d}^2\bar{\xi}/\mathrm{d}\bar{x}^2$ is involved both in the resistive diffusion of $B_{1x}$ and the Hall effects; the differences between equations (54) and (55) identify the terms related to the diffusion of $B_{1x}$. The detailed analysis of each of the six parametric regions (PR1, ..., PR6) amenable to asymptotic reduction follows next.

### *4.1. Weak-Hall regime (PR1)*

The regime to be labeled PR1 spans the asymptotic region where Hall effects are negligible, which corresponds to $\sigma^2 \ll 1$ or $\sigma^2 \ll \tau$. There, a solution with $\bar{x} \sim 1$, $\bar{\xi} \sim 1$ and $\bar{Q} \ll 1$ is obtained. Hence, the contribution of $B_{1z}$ is negligible and the inner tearing mode system reduces to the classic single-fluid equation [1], independent of $\sigma$ and $\tau$:

$$\mathrm{d}^2\bar{\xi}/\mathrm{d}\bar{x}^2 - \bar{x}^2\bar{\xi} = -\bar{x}, \tag{56}$$

whose well-known solution is the parabolic cylinder function [1, 9] $\xi(\bar{x}) = U(0,\bar{x}) \equiv F(\bar{x})$:

$$F(\bar{x}) = \frac{\bar{x}}{2}\int_0^1 \mathrm{d}\mu(1-\mu^2)^{-1/4}\mathrm{e}^{-\mu\bar{x}^2/2}. \tag{57}$$

The corresponding dispersion relation, to be discussed in section 5, is the same as in the single-fluid theory [1].

### *4.2. General high-beta regime (PR2)*

This region corresponds to sufficiently high values of $\beta$ to make $\tau \ll 1$, so that with a negligible $\tau$ the results become independent of $\beta$, compressible effects remain negligible and the length scale associated with two-fluid effects is the ion skin depth $d_\mathrm{i}$. The two-fluid tearing system depends only on the parameter $\sigma$, which is here assumed to be arbitrary and formally ordered as $\sigma = O(1)$.

The inner tearing mode system for this regime is the $\tau \to 0$ limit of our equations (50) and (51):

$$\frac{\mathrm{d}^2\bar{\xi}}{\mathrm{d}\bar{x}^2} = \bar{x}^2(\bar{\xi}+\bar{Q}) - \bar{x}, \tag{58}$$

$$\frac{\mathrm{d}^2\bar{Q}}{\mathrm{d}\bar{x}^2} - \sigma^2\frac{\mathrm{d}^2\bar{\xi}}{\mathrm{d}\bar{x}^2} = \bar{x}^2\bar{Q}, \tag{59}$$

which indicates that the resistive diffusions of both $B_{1x}$ and $B_{1z}$ are relevant. This system is diagonalized by the eigenfunction linear combinations

$$V_n = \bar{\xi} + a_n\bar{Q}, \qquad n = 1, 2 \tag{60}$$

with

$$a_n(\sigma) = \frac{1}{2} + \frac{(-1)^n}{2}\left(1+\frac{4}{\sigma^2}\right)^{1/2}, \tag{61}$$

in terms of which it becomes

$$\frac{1}{\lambda_n}\frac{\mathrm{d}^2V_n}{\mathrm{d}\bar{x}^2} = \bar{x}^2V_n - \bar{x}, \tag{62}$$

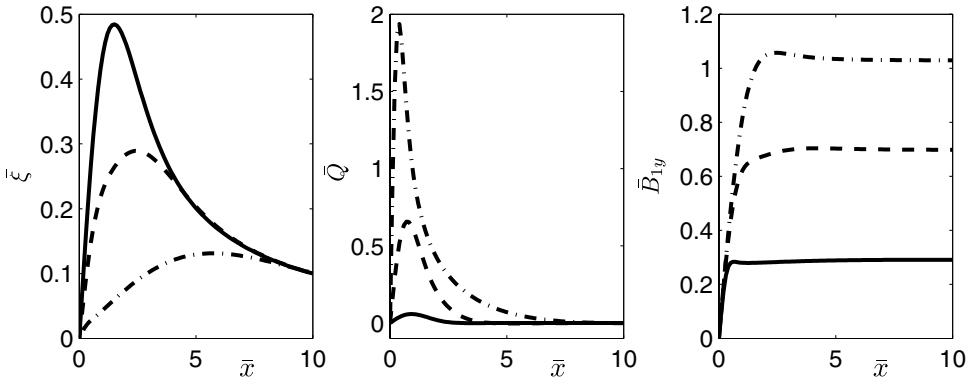


**Figure 3.** Inner solution for PR2 and $\sigma = 0.6$ (solid), 3 (dashed) and 15 (dash-and-dot). Notice that $\bar{x}\bar{Q} < 0$ for $|\bar{x}| \gg 1$, equation (52). Here and in the next figure, $\bar{B}_{1y} = -\mathrm{i}B_{1y}/B_{1x}(0)\times\epsilon_\eta/(\epsilon_\gamma k d_0)$.

where the eigenvalues $\lambda_n$ are

$$\lambda_n(\sigma) = 1 + \sigma^2 a_n(\sigma) \tag{63}$$

and satisfy $\lambda_1\lambda_2 = 1$. From equation (52), the boundary conditions for $V_n$ are $V_n(0) = 0$ and $V_n(|\bar{x}| \gg 1) = \bar{x}^{-1} + O(\bar{x}^{-5})$. Upon rescaling of the variables with appropriate powers of $\lambda_n$, this problem becomes mathematically identical to the canonical single-fluid one, equation (56), and has therefore the solution

$$V_n(\bar{x}) = \lambda_n^{1/4} F(\lambda_n^{1/4}\bar{x}) \tag{64}$$

with $F$ defined in equation (57). Then, the solutions for $\bar{\xi}$ and $\bar{Q}$ are

$$\bar{\xi}(\bar{x}) = \frac{a_1\lambda_2^{1/4}F(\lambda_2^{1/4}\bar{x}) - a_2\lambda_1^{1/4}F(\lambda_1^{1/4}\bar{x})}{a_1 - a_2}, \tag{65}$$

$$\bar{Q}(\bar{x}) = \frac{\lambda_1^{1/4}F(\lambda_1^{1/4}\bar{x}) - \lambda_2^{1/4}F(\lambda_2^{1/4}\bar{x})}{a_1 - a_2}. \tag{66}$$

Figure 3 shows these inner solutions for $\bar{\xi}$, $\bar{Q}$ and the resulting $\bar{B}_{1y}$, for three different values of $\sigma$. For $\sigma \ll 1$ we recover the result of the weak-Hall regime and for $\sigma \gg 1$ we enter the strong-Hall, high-beta regime PR3 to be discussed next. Based on this solution, we will obtain in section 5 a novel high-beta dispersion relation valid for arbitrary values of the Hall parameter, whose asymptotes are the single-fluid dispersion relation [1] in the weak-Hall limit and a dispersion relation identical to the one obtained, under different assumptions, with the so-called electron-MHD model [3, 4] in the strong-Hall limit.

### *4.3. Strong-Hall, high-beta regime (PR3)*

This parametric region is defined by the conditions $\sigma \gg 1$ and $\tau \ll \sigma$, corresponding to the large-$\sigma$ or strong-Hall limit of the previous high-beta regime PR2. For $\sigma \gg 1$, equations (61), (63), (65) and (66) show that the non-ideal boundary layer splits into two distinct asymptotic sublayers: an innermost sublayer of width $d_1 = d_0\lambda_1^{-1/4} = d_0\sigma^{-1/2}$ and an intermediate sublayer of width $d_2 = d_0\lambda_2^{-1/4} = d_0\sigma^{1/2}$, that is

$$d_1 = \sqrt{L_B d_\eta/(k d_\mathrm{i})}, \qquad d_2 = \sqrt{L_B d_\gamma k d_\mathrm{i}}. \tag{67}$$

These expressions make clear the role of the ion skin depth, $d_i$, in separating these two scales. The absence of $d_\eta$ in $d_2$ is a hint that the intermediate layer is non-resistive.

Although the general solution given by equations (65) and (66) contains this strong-Hall limit where the two sublayers separate, it is useful to show explicitly the asymptotic models for each of these sublayers. In the intermediate sublayer where the resistive diffusion of both $B_{1z}$ and $B_{1x}$ is negligible, the scaling of variables is

$$\bar{x}^{-1} \sim \bar{Q} \sim \bar{\xi} \sim \sigma^{-1/2} \tag{68}$$

and the reduced system is the $\tau \to 0$ limit of equation (54):

$$\sigma^2 \frac{\mathrm{d}^2\bar{\xi}}{\mathrm{d}\bar{x}^2} = \bar{x}^2\bar{\xi} - \bar{x} = -\bar{x}^2\bar{Q}. \tag{69}$$

In the innermost sublayer, the scaling of the variables is

$$\bar{x}^{-1} \sim \bar{Q} \sim \sigma^{1/2}, \qquad \bar{\xi} \ll \bar{Q} \tag{70}$$

Then, the dominant contribution to the tearing mode reduces here to

$$\mathrm{d}^2\bar{Q}/\mathrm{d}\bar{x}^2 = \sigma^2(\bar{x}^2\bar{Q} - \bar{x}) \tag{71}$$

and $\bar{\xi}$ does not contribute to the leading order dispersion relation. Nonetheless, $\mathrm{d}^2\bar{\xi}/\mathrm{d}\bar{x}^2$, which provides $B_{1x}$ diffusion, is not negligible within this sublayer.

Thus, in contrast to the weak-Hall regime where $\bar{Q}$ is negligible and $\bar{\xi}$ is bounded by the diffusion of $B_{1x}$, in this PR3 regime the $B_{1x}$ diffusion is negligible in the intermediate sublayer where the Hall effects give rise to $\bar{Q}$ and bound $\bar{\xi}$. However, the intermediate sublayer solution for $\bar{Q}$, equation (69), is unbounded as $\bar{x} \to 0$. This is regularized by the diffusion of $B_{1x}$ and $B_{1z}$ in the innermost, resistive sublayer governed by equation (71). As mentioned earlier, the dispersion relation to be found for this high-beta, strong-Hall regime will turn out to be the same as the one obtained in a different context with the so-called electron-MHD model [3, 4].

### *4.4. General strong-Hall regime (PR4)*

The parametric region labeled (PR4) corresponds to $\tau \sim \sigma \gg 1$ and has been studied by Mirnov *et al* [2] for $\epsilon_B \ll 1$. This regime preserves the same scaling of variables as in PR3, with two sublayers having the characteristic widths defined in equation (67). The intermediate layer has the scalings of equation (68) and is governed by equation (54). Following the Fourier transform method of [8], that equation admits a solution in terms of parabolic cylinder functions [9],

$$\bar{\xi}(\bar{x}) = \frac{1}{\bar{x}} - \bar{Q}(\bar{x}) = \frac{1-\sigma}{2\sigma}\int_0^{+\infty} \mathrm{d}k\ \sin k\bar{x}\,\frac{U(\tau/2\sigma, \sqrt{2\sigma}k)}{U(\tau/2\sigma, 0)} + \tau\int_0^{+\infty} \mathrm{d}k\,\frac{\sin\ k\bar{x}}{\tau + k^2\sigma^2}. \tag{72}$$

The scalings of equation (70) hold in the innermost resistive layer, where the governing equation becomes

$$\mathrm{d}^2\bar{Q}/\mathrm{d}\bar{x}^2 = (\sigma^2\bar{x}^2 + \tau)\bar{Q} - \sigma^2\bar{x} \tag{73}$$

and the resistive layer solution is [2]

$$\bar{Q}(\bar{x}) = \sigma\int_0^{+\infty} \mathrm{d}k\ \sin\ k\bar{x}\,\frac{U(\tau/2\sigma, \sqrt{2\sigma}k)}{U(\tau/2\sigma, 0)}. \tag{74}$$

Again $\bar{\xi} \ll \bar{Q}$ and does not contribute to the dispersion relation. The $\tau \ll \sigma$ and $\tau \gg \sigma$ limits of these solutions correspond, respectively, to the previous PR3 and to the strong-Hall, low-beta parametric regime PR5 to be considered next.

*4.5. Strong-Hall, low-beta regime (PR5)*

This regime is defined by the conditions $1 \ll \sigma \ll \tau \ll \sigma^2$. Here, the $\tau \gg \sigma$ limit produces qualitative changes in the PR4 solution and the lengths of the intermediate and resistive sublayers become, respectively

$$d_2 = d_s, \qquad d_1 = \frac{L_B\sqrt{d_\gamma d_\eta}}{d_s}, \tag{75}$$

where $d_s = d_i\sqrt{\beta}$ is the ion sound gyroradius. The scaling of variables in the intermediate, non-diffusive layer of PR5 is

$$\bar{x}^{-1} \sim \bar{Q} \sim \bar{\xi} \sim \tau^{1/2}\sigma^{-1} \tag{76}$$

and system (54) reduces to

$$\frac{\mathrm{d}^2\bar{\xi}}{\mathrm{d}\bar{x}^2} = \frac{\tau}{\sigma^2}\left(\bar{\xi} - \frac{1}{\bar{x}}\right) = -\frac{\tau}{\sigma^2}\bar{Q}, \tag{77}$$

which has the solution

$$\bar{\xi}(\bar{x}) = \frac{1}{\bar{x}} - \bar{Q}(\bar{x}) = \tau\int_0^{+\infty} \mathrm{d}k \frac{\sin\, k\bar{x}}{\tau + k^2\sigma^2}. \tag{78}$$

The innermost, resistive layer has the scalings

$$\bar{x}^{-1} \sim \bar{Q} \sim \tau^{-1/2}\sigma, \qquad \bar{\xi} \ll \bar{Q}, \tag{79}$$

which make the $\mathrm{d}^2\bar{Q}/\mathrm{d}\bar{x}^2$ term of equation (73) negligible, leading to the simple solution

$$\bar{Q} = \frac{\sigma^2\bar{x}}{\sigma^2\bar{x}^2 + \tau}. \tag{80}$$

Thus, the intermediate layer solution here has the same features as the one found in PR3 and PR4: $\bar{\xi}$ remains bounded by $\bar{Q}$, which is now triggered by Hall and compressibility effects and is unbounded in its small $\bar{x}$ limit. On the other hand, the behavior of the resistive layer of PR5 is peculiar. The $\mathrm{d}^2\bar{Q}/\mathrm{d}\bar{x}^2$ term in equation (73), which represents the resistive diffusion of $B_{1z}$, is negligible and $\bar{Q}$ is regularized by a combination of compressibility and $B_{1x}$-diffusion. The latter manifests itself through the term $\tau$ in the denominator of equation (80), absent in equation (77). This strong-Hall, low-beta regime is the only case with two distinct sublayers but negligible $B_{1z}$-diffusion.

A unified treatment of the two sublayers relevant to this low-beta, strong-Hall regime is possible once we know that the $B_{1z}$-diffusion is negligible and that the defining conditions and $\bar{x}$ scalings (equations (76) and (79)) of PR5 guarantee that $\sigma^2 \gg 1$ and $\tau \gg \bar{x}^2$ through the two sublayers. Then, the $\sigma^2 \gg 1$ and $\tau \gg \bar{x}^2$ limit of equation (55),

$$\frac{\mathrm{d}^2\bar{\xi}}{\mathrm{d}\bar{x}^2} = \frac{\bar{x}^2\bar{\xi} - \bar{x}}{(\sigma^2/\tau)\bar{x}^2 + 1} = -\frac{\tau}{\sigma^2}\bar{Q}, \tag{81}$$

provides the unified system that covers the two previously given sublayer systems of equations (77) and (80). Equation (81) is the 'constant-$B_{1x}$ (constant-$\psi$) approximation' version of the system considered by Kuvshinov [7] in his study of the so-called semicollisional tearing modes. In our case, the separation into two distinct asymptotic sublayers is a consequence of the smallness of $\tau/\sigma^2$ and leads to the much simpler solution (80) in the innermost sublayer, which will still yield the same semicollisional tearing mode dispersion relation.

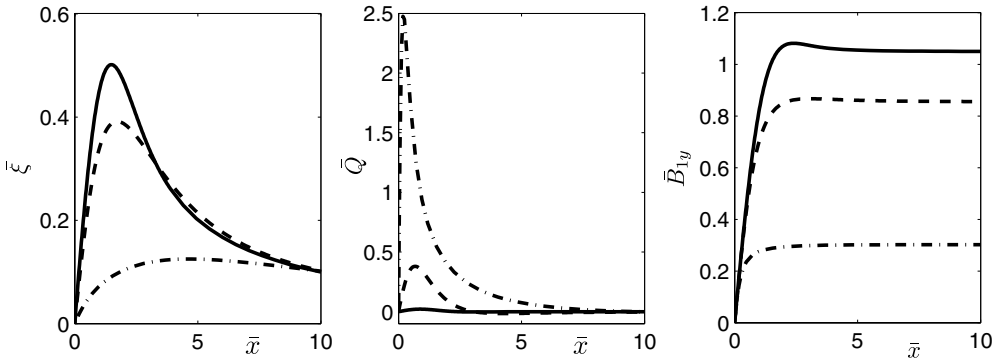


**Figure 4.** Inner solution for PR6 and $\sigma\tau^{-1/2} = 0.2$ (solid), 1 (dashed) and 5 (dash-and-dot).

### *4.6. General low-beta regime (PR6)*

This regime corresponds to $\tau \sim \sigma^2 \gg 1$, with the scalings $\bar{x} \sim \bar{\xi} \sim \bar{Q} \sim 1$. Accordingly, the inner region consists of a single layer governed by the system given in equation (81), with the parameter $\tau/\sigma^2$ as well as all the variables ordered as comparable to unity. At the asymptotic ends of this regime, the $\tau/\sigma^2 \ll 1$ limit corresponds to the previously discussed PR5 where the inner region separates into two distinct sublayers, and the $\tau/\sigma^2 \to \infty$ (hence $\bar{Q} \to 0$) limit corresponds to the weak-Hall regime governed by equation (56). Therefore, the PR6 regime provides the continuous transition between PR5 and PR1, which completes our covering of the parameter space.

An analytic solution of equation (81) in terms of standard mathematical functions appears to be unavailable when $\tau/\sigma^2 \sim 1$. Instead, we have carried out a direct numerical integration (matching the simple asymptotic behavior at $\bar{x} \gg 1$) and figure 4 shows the solutions for three different values of $\tau/\sigma^2$.

## 5. The dispersion relation

Once $\bar{\xi}$ and $\bar{Q}$ are known, the integration of equation (41) yields

$$\frac{\mathrm{d}B_{1x}}{\mathrm{d}x} = B_{1x}(0)k^2 d_0 \frac{\epsilon_\gamma}{\epsilon_\eta} \int_0^{x/d_0} (1 - \bar{x}\bar{\xi} - \bar{x}\bar{Q})\,\mathrm{d}\bar{x} \tag{82}$$

and the asymptotic matching of this result with equation (36) yields the dispersion relation

$$k^{-1}\Delta' = \epsilon_\gamma^{5/4}\epsilon_\eta^{-3/4}(kL_B)^{1/2} D(\sigma, \tau), \tag{83}$$

where

$$D(\sigma, \tau) = \int_{-\infty}^{+\infty} (1 - \bar{x}\bar{\xi} - \bar{x}\bar{Q})\,\mathrm{d}\bar{x}. \tag{84}$$

Equation (83) specifies the dimensionless normalized growth rate $\epsilon_\gamma$ as an implicit function of the five dimensionless input parameters $\epsilon_\eta$, $\alpha$, $\beta$, $kL_B = \epsilon_B^{-1}kL$ and $k^{-1}\Delta'(kL)$:

$$\frac{\epsilon_\gamma^{5/4}(kL_B)^{1/2}}{\epsilon_\eta^{3/4}k^{-1}\Delta'}\, D\left(\frac{\epsilon_\gamma^{1/2}\alpha}{\epsilon_\eta^{1/2}}, \frac{\epsilon_\gamma^{3/2}kL_B(1+\beta)}{\epsilon_\eta^{1/2}\beta}\right) = 1. \tag{85}$$

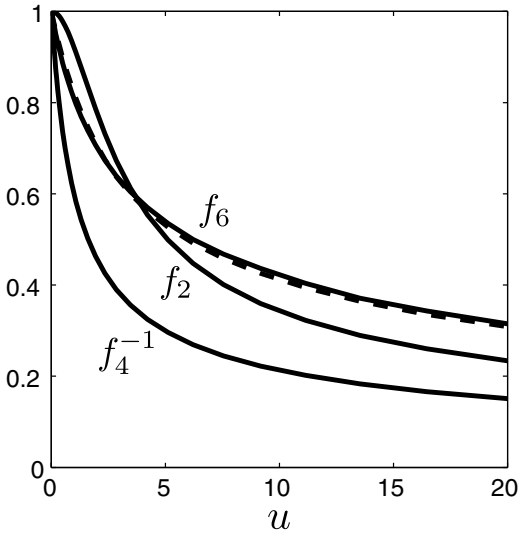


**Figure 5.** Functions $f_2(u)$, $1/f_4(u)$ and $f_6(u)$. The dashed line is the approximate fit of $f_6$ in equation (89).

The inner layer solutions for $\bar{\xi}(\bar{x})$ and $\bar{Q}(\bar{x})$ obtained in the previous section allow us to derive the different expressions of the dispersion function $D(\sigma, \tau)$, equation (84), that apply in the different parametric regions. In the weak-Hall regime PR1, $D(\sigma, \tau)$ is constant:

$$D(\sigma, \tau) = \int_{-\infty}^{+\infty} [1 - yF(y)]\, \mathrm{d}y = \frac{2\pi\Gamma(3/4)}{\Gamma(1/4)} \equiv C \simeq 2.12. \tag{86}$$

In the general high-beta regime PR2, the dispersion function takes the form $D(\sigma, \tau) = Cf_2(\sigma)$, where

$$f_2(\sigma) = \frac{a_1\lambda_1^{-1/4} - a_2\lambda_2^{-1/4}}{a_1 - a_2},$$

and $a_n(\sigma)$ and $\lambda_n(\sigma)$ are specified in equations (61) and (63). Substituting these, we get the explicit form

$$f_2(\sigma) = \frac{1}{2}\sum_{n=1}^{2}\left[1 + (-1)^n\left(1 + 4/\sigma^2\right)^{-1/2}\right]\left[1 + \sigma^2/2 + (-1)^n\sigma\left(1 + \sigma^2/4\right)^{1/2}\right]^{-1/4}. \tag{87}$$

The function $f_2(\sigma)$ is plotted in figure 5. We have $f_2(0) = 1$ which corresponds to the overlapping with PR1, $f_2(1) = 0.92$, and $f_2(\sigma \gg 1) \simeq \sigma^{-1/2}$ which corresponds to the overlapping with PR3. In PR3 where $\sigma \gg 1$, the contribution to the dispersion function of the innermost resistive layer is of order $\sigma^{-1/2}$ and dominates over the contribution of the intermediate layer of order $\sigma^{-3/2}$. In this sense, it can be said that the tearing mode growth in PR3 is dominated by the $B_{1z}$-diffusion.

In order to determine the dispersion function in PR4 (and PR5) we take into account the fact that the dominant contribution comes from the innermost resistive layer. Then, using equation (74),

$$1 - \bar{x}\bar{\xi} - \bar{x}\bar{Q} \simeq 1 - \bar{x}\bar{Q} = \sqrt{2\sigma}\int_0^{\infty} \cos\, k\bar{x}\,\frac{U'(\tau/2\sigma, \sqrt{2\sigma}k)}{U(\tau/2\sigma, 0)}\,\mathrm{d}k,$$

which yields $D(\sigma,\tau)=C\sigma^{-1/2}f_4(\tau/\sigma)$ with

$$f_4(u)=-\frac{\sqrt{2}\pi}{C}\frac{U'(u/2,0)}{U(u/2,0)}=\frac{2\pi}{C}\frac{\Gamma[(3+u)/4]}{\Gamma[(1+u)/4]}. \tag{88}$$

Figure 5 depicts the function $f_4(u)$. We have $f_4(0)=1$, which corresponds to the overlapping with PR3, and $f_4(u\gg 1)\simeq \pi\sqrt{u}/C$ which corresponds to the overlapping with PR5.

In PR6, the dispersion function takes the form $D(\sigma,\tau)=C\ f_6(\sigma^2/\tau)$, where the function $f_6(u)$ is obtained numerically and is shown in figure 5, together with the approximate, simple fit

$$f_6(u)\simeq\frac{1-u/4+\pi u^2/20}{1+Cu^{5/2}/20}. \tag{89}$$

We have $f_6(0)=1$, which corresponds to the overlapping with PR1 and $f_6(u\gg 1)=\pi/(C\sqrt{u})$ which corresponds to the overlapping with PR5.

The simple asymptotic expressions of $f_2$, $f_4$ and $f_6$ for small and large arguments allow us to recover explicit forms of the dispersion relation in PR1, PR3 and PR5. Thus, in the weak-Hall regime PR1 we have

$$\epsilon_\gamma=\epsilon_\eta^{3/5}\left(\frac{\epsilon_B\Delta'^2}{C^2k^3L}\right)^{2/5}, \tag{90}$$

which coincides with the classic single-fluid dispersion relation [1]. In the strong-Hall, high-beta regime PR3 we have

$$\epsilon_\gamma=\epsilon_\eta^{1/2}\left(\alpha\,\frac{\epsilon_B\Delta'^2}{C^2k^3L}\right)^{1/2}, \tag{91}$$

which coincides with the dispersion relation obtained with the so-called electron-MHD model [3, 4]. Finally, in the strong-Hall, low-beta regime PR5 (where $\beta\ll 1$) we have

$$\epsilon_\gamma=\epsilon_\eta^{1/3}\left(\alpha\beta^{1/2}\,\frac{\epsilon_B\Delta'}{\pi k^2L}\right)^{2/3}, \tag{92}$$

which coincides with the so-called semicollisional tearing mode dispersion relation [5–7]. We recall that $\alpha=kd_\mathrm{i}$ and $\alpha\beta^{1/2}=kd_\mathrm{s}$, so the characteristic lengths associated with two-fluid effects in PR3 and PR5 are, respectively, the ion skin depth and the ion sound gyroradius. The complete functions $f_2$, $f_4$ and $f_6$ provide the smooth connections between these three classic dispersion relations in the transitional regimes PR2, PR4 and PR6. The exact analytic result for PR2 is a novel contribution of this work and it has been used in a recent benchmark of the state of the art two-fluid code NIMROD [10], showing excellent agreement with the numerics. The result for PR4 coincides with the corresponding analytic result derived in [2] assuming a strong magnetic guide field ($\epsilon_B\ll 1$), but is shown here to apply also for $\epsilon_B\sim 1$. The transition between the semicollisional and single-fluid dispersion relations in PR6 is not covered by the analyses of either [2] or [7] and our semi-analytic solution for this regime is also new.

## 6. Concluding discussion

The complete form of the general dispersion relation equation (85) involves only three independent combinations of the eigenvalue $\epsilon_\gamma$ and the five dimensionless input parameters of

the problem. It is therefore appropriate to introduce

$$\hat{\gamma} = \frac{\epsilon_\gamma}{\epsilon_\eta^{3/5}} \left( \frac{C^2 k^3 L}{\epsilon_B \Delta'^2} \right)^{2/5}, \quad \hat{\alpha} = \frac{\alpha}{\epsilon_\eta^{1/5}} \left( \frac{\epsilon_B \Delta'^2}{C^2 k^3 L} \right)^{1/5}, \quad \hat{\beta} = \frac{\beta}{\epsilon_\eta^{2/5}(1+\beta)} \left( \frac{C^8 \epsilon_B k^2}{\pi^5 L \Delta'^3} \right)^{2/5}, \tag{93}$$

as the naturally scaled growth rate output and the two naturally scaled input parameters, respectively. In terms of these, the general dispersion relation (85) assumes the simple reduced form

$$\hat{\gamma}^{5/4} \, D\left( \hat{\gamma}^{1/2} \hat{\alpha}, \frac{C^2 \hat{\gamma}^{3/2}}{\pi^2 \hat{\beta}} \right) = C, \tag{94}$$

and either explicit or implicit asymptotic expressions for $\hat{\gamma}(\hat{\alpha}, \hat{\beta})$ in the different parametric regimes are

$$\begin{aligned}
&\hat{\gamma} = 1 && \text{in PR1,} \\
&\hat{\gamma} = f_2^{-4/5}(\hat{\gamma}^{1/2}\hat{\alpha}) && \text{in PR2,} \\
&\hat{\gamma} = \hat{\alpha}^{1/2} && \text{in PR3,} \\
&\hat{\gamma} = \hat{\alpha}^{1/2} f_4^{-1}\left( \frac{C^2 \hat{\gamma}}{\pi^2 \hat{\beta} \hat{\alpha}} \right) && \text{in PR4,} \\
&\hat{\gamma} = \hat{\alpha}^{2/3} \hat{\beta}^{1/3} && \text{in PR5,} \\
&\hat{\gamma} = f_6^{-4/5}\left( \frac{\pi^2 \hat{\beta} \hat{\alpha}^2}{C^2 \hat{\gamma}^{1/2}} \right) && \text{in PR6.}
\end{aligned} \tag{95}$$

Once the growth rate has been solved for, the different parametric region boundaries (that were initially established in terms of the mathematical scaling parameters $\sigma$ and $\tau$) can now be defined in terms of the primary input parameters $\hat{\alpha}$ and $\hat{\beta}$ alone. The result is given in table 2 and shown graphically in figure 6. The physical properties of the inner region in the different parametric regions are summarized in table 2 too. Thus, Hall effects are relevant in PR2 to PR6, and compressibility effects in PR4 to PR6. Diffusion of $B_{1x}$ is a dominant mechanism in all parametric regions and diffusion of $B_{1z}$ is an additional dominant mechanism in PR2 to PR4. The comparison between $\bar{Q}(\bar{x})$, related to $B_{1z}$, and the displacement $\xi(\bar{x})$ in the resistive sublayer and the dispersion relation shows that $\bar{Q}(\bar{x})$ dominates in the strong-Hall regions, PR3 to PR5; $\xi(\bar{x})$ dominates in the weak-Hall region PR1; and our novel solutions for PR2 and PR6 cover the weak-to-strong Hall transitions (at high- and low-beta, respectively) where $\bar{\xi}$ and $\bar{Q}$ are of the same order.

Except for $kL$ close to one, the tearing instability index, equation (37), can be approximated by $k^{-1}\Delta' \simeq 2(kL)^{-2}$. Using this approximation and also $\beta/(1+\beta) \simeq \beta$, table 3 provides scaling laws for the tearing mode growth rate and the widths of the whole non-ideal region and the resistive sublayer. There, taking into consideration the boundaries of the region PR5 we get $(d_2/L)|_{\text{PR3}} \ll (d_2/L)|_{\text{PR5}} \ll (d_2/L)|_{\text{PR1}}$, so that the width of the whole non-ideal region does tend to zero when $\epsilon_\eta \to 0$ in all cases.

In order to complete our analysis, the parametric boundaries of validity of our reduced model, equations (45) and (46), must be determined. First, the overall boundary set by our general subsonic growth condition, $\beta \gg \epsilon_\gamma^2$, can now be explicited in the space of primary input parameters and is given in table 3. In terms of the unscaled $\alpha = kd_\text{i}$, $\beta = c_\text{s}^2/c_\text{A}^2$, and the inverse magnetic Reynolds number $\epsilon_\eta$ (and taking as always $kL_B \sim k^{-1}\Delta' \sim 1$), the tearing mode is subsonic: always in PR2; for $\beta \gg \epsilon_\eta^{6/5}$ in PR1 and PR6; for $\beta \gg \epsilon_\eta^2 \alpha^4$ in

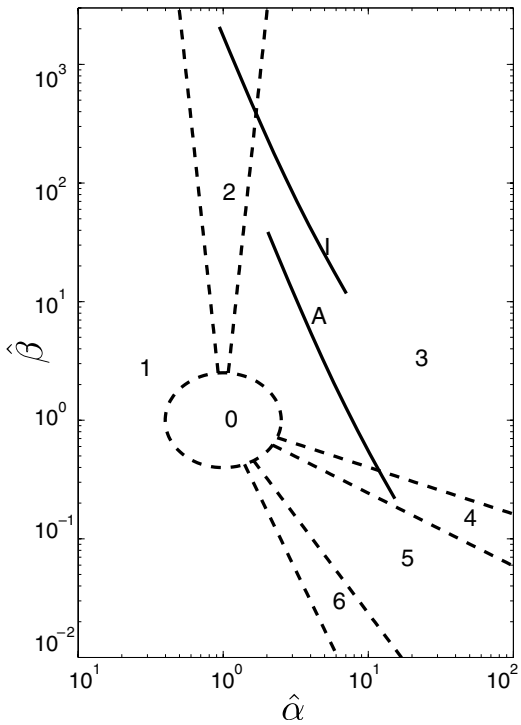


**Figure 6.** Dashed lines indicate the boundaries of the different parametric regions in the plane of primary input parameters. Solid lines show the location of plasmas A and I of table 1 for $k^{-1}\Delta'$ ranging from 0.1 (top) to 10 (bottom).

**Table 3.** Scaling laws for the growth rate, the widths of the inner layers and the subsonic range in PR1, PR3 and PR5. The extension of these laws to the intermediate regions PR2, PR4 and PR6, by patching where they intersect, is straightforward. Recall $kd_\mathrm{i} = \alpha$, $kd_\mathrm{s} = \alpha\beta^{1/2}$ and $k^{-1}\Delta' \sim 2(kL)^{-2}$.

| | PR1 | PR3 | PR5 |
|---|---|---|---|
| $\epsilon_\gamma \sim$ | $\epsilon_\eta^{3/5}\epsilon_B^{2/5}(kL)^{-2}$ | $\epsilon_\eta^{1/2}(kd_\mathrm{i})^{1/2}\epsilon_B^{1/2}(kL)^{-5/2}$ | $\epsilon_\eta^{1/3}(kd_\mathrm{s})^{2/3}\epsilon_B^{2/3}(kL)^{-2}$ |
| $d_2/L \sim$ | $\epsilon_\eta^{2/5}\epsilon_B^{-2/5}(kL)^{-1}$ | $\epsilon_\eta^{1/4}(kd_\mathrm{i})^{3/4}\epsilon_B^{-1/4}(kL)^{-7/4}$ | $d_\mathrm{s}/L$ |
| $d_1/L \sim$ | $d_2/L$ | $\epsilon_\eta^{1/2}(kd_\mathrm{i})^{-1/2}\epsilon_B^{-1/2}(kL)^{-1/2}$ | $\epsilon_\eta^{2/3}(kd_\mathrm{s})^{-2/3}\epsilon_B^{-2/3}(kL)^{-1}$ |
| $\beta \gg$ | $\epsilon_\eta^{6/5}\epsilon_B^{4/5}(kL)^{-4}$ | $\epsilon_\eta(kd_\mathrm{i})\epsilon_B(kL)^{-5}$ | $\epsilon_\eta^2(kd_\mathrm{i})^4\epsilon_B^4(kL)^{-12}$ |

PR5; for $\beta \gg \epsilon_\eta^{2/3}$ in PR4; for $\beta \gg \epsilon_\eta\alpha$ in PR3. Thus, the tearing mode is subsonic in all the parametric space except for extremely low values of $\beta$ or very large values of the Hall parameter $\alpha$. Second, we have checked (for $kL_B \sim k^{-1}\Delta' \sim 1$) the subsonic condition to be *necessary and sufficient* to neglect the imaginary terms dropped in the derivation of our basic inner region model, equations (45) and (46), hence to keep the growth rate purely real. Therefore, the real-to-complex transition of the growth rate is expected to occur at the sonic range. Future work based on the full inner model, equations (40)–(43), could address whether the growth rate is effectively complex in the cold-plasma and very-strong-Hall limits.

Both the parametric location and the growth rate of the tearing mode depend on $\epsilon_B$ and $k^{-1}\Delta'$. Considering the dependence on $\epsilon_B$, $\hat{\beta}$ and $\hat{\alpha}^2$ are proportional to $\epsilon_B^{2/5}$ and $\epsilon_\gamma$

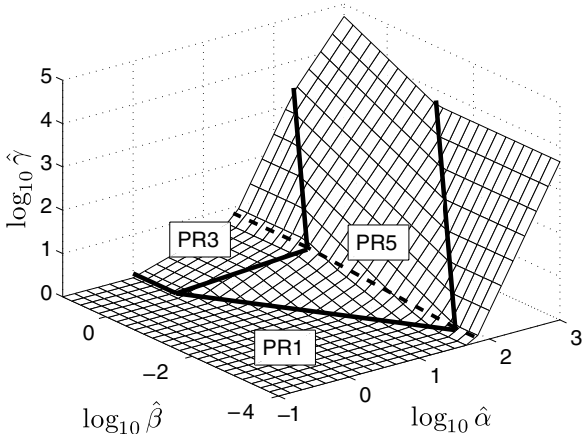


**Figure 7.** Growth rate of the tearing mode, $\hat{\gamma}(\hat{\alpha}, \hat{\beta})$, in the different parametric regions for the resistive and collisionless regimes, for $m_\mathrm{i}/m_\mathrm{e} = 3672$. For illustration purposes, regions PR2, PR4 and PR6 have been reduced to solid lines, and the resistive-to-collisionless transition region to a dashed line.

is proportional to $\epsilon_B^{2/5}\hat{\gamma}(\hat{\alpha}, \hat{\beta})$ so that the parametric space point tends to move towards PR3 as $\epsilon_B$ increases. Therefore, the two-fluid theory is more appropriate for $\epsilon_B = O(1)$. Considering the dependence on $k^{-1}\Delta'$, $\hat{\beta}$ and $\hat{\alpha}^{-2}$ are both proportional to $k\Delta'^{-1}$ and $\epsilon_\gamma$ is proportional to $k^{-1}\Delta'\hat{\gamma}(\hat{\alpha}, \hat{\beta})$. Therefore, as $k^{-1}\Delta'$ increases, $\hat{\beta}\hat{\alpha}^2$ remains constant and the parametric space point either remains always in PR1, moves from PR1 to PR6 through PR0, or moves from PR1 to PR5 through PR3. This last case is favored except at very low $\beta$ and is illustrated in figure 6 for the two plasmas of table 1. Notice that our solution from PR1 to PR3 through PR2 (equations (65), (66) and (87)) covers well the $k^{-1}\Delta' = O(1)$ range for these plasmas.

Our analysis has been self-limited to values of the instability index of order unity, $k^{-1}\Delta' = O(1)$. Nonetheless, results here can be extended to moderately large values of the instability index, as long as: (i) the constant $B_{1x}$-approximation is valid, which requires that $d_2\Delta' \sim (d_2/L)(kL)^{-1} \ll 1$; (ii) the growth rate is subsonic and (iii) the imaginary terms in the inner region model that can make the growth rate complex are negligible. Limitations on $k^{-1}\Delta'$ for the first and second conditions are readily obtained from table 3; the coincidence of the third and second conditions for $k^{-1}\Delta' \gg 1$ is to be checked in each case.

Finally, the extension of the tearing mode analysis to include the finite electron inertia effect is detailed in the appendix. Figure 7 depicts the surface representing the scaled growth rate $\hat{\gamma}(\hat{\alpha}, \hat{\beta})$ covering both the resistive and collisionless regimes. The finite electron mass increases the tearing mode growth rate relative to its massless limit, this effect becoming significant when $\hat{\alpha}^2\hat{\gamma}(\hat{\alpha}, \hat{\beta}) \geqslant O(m_\mathrm{i}/m_\mathrm{e})$ which points mainly to the strong-Hall regimes. Figure 8 plots the sonic boundary of the tearing mode for different plasmas resistivities, showing that the growth rate becomes sonic within resistive or collisionless regimes depending on the relative values of $\epsilon_\eta$ and $m_\mathrm{e}/m_\mathrm{i}$.

## Acknowledgments

The stay of E Ahedo at the Massachusetts Institute of Technology was sponsored by the Ministerio de Ciencia e Innovación of Spain under Project ESP2007-62694. The work of J J Ramos was sponsored by the US Department of Energy under Grants Nos

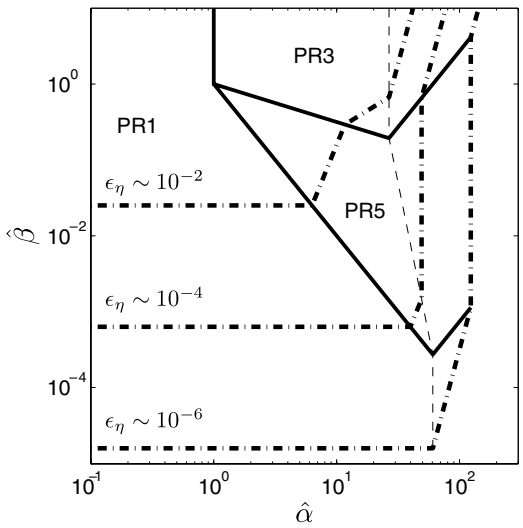


**Figure 8.** Dash-and-dot lines show the location of the sonic range of the tearing mode for three plasma resistivities, $m_\mathrm{i}/m_\mathrm{e} = 3672$, and $kL_B \sim k^{-1}\Delta' \sim 1$. The subsonic range where the present analysis applies is above and to the left of those lines. As in figure 7, regions PR2, PR4 and PR6 and the resistive-to-collisionless transition have been reduced to solid and dashed lines, respectively.

DEFG02-91ER54109 and DEFC02-08ER54969 at the Massachusetts Institute of Technology and as part of the author's participation in the Center for Extended MHD Modeling (CEMM).

## Appendix. Generalization for finite electron inertia

The effect of a finite but realistically small electron mass on the linear theory of the tearing mode amounts to just a slight modification of the massless electron theory presented in the main body of this paper. Due to the small electron to ion mass ratio, $\mu = m_\mathrm{e}/m_\mathrm{i} \ll 1$, only the inertial contribution to the electron momentum conservation equation in the non-ideal boundary layer, which like the resistive diffusivity has the character of a singular perturbation capable of breaking the magnetic frozen-in law, is of significance. So, the only modification needed in the linearized system (11)–(16) is to use, instead of equation (13),

$$\boldsymbol{E}_1 = -\boldsymbol{v}_1 \times \boldsymbol{B}_0 + \eta \boldsymbol{j}_1 + \frac{m_\mathrm{i}}{e}\left(\frac{\partial \boldsymbol{v}_1}{\partial t} + \frac{\nabla p_{i1}}{\rho_0}\right) + \frac{m_\mathrm{e}}{e^2 n_0}\frac{\partial \boldsymbol{j}_1}{\partial t}. \tag{A.1}$$

Therefore, the linear tearing mode results derived for zero electron mass, can be generalized to finite electron mass simply by substituting $\eta + \gamma m_\mathrm{e}/(e^2 n_0)$ for $\eta$, that is $\epsilon_\eta + \epsilon_\gamma k^2 d_\mathrm{e}^2$ for $\epsilon_\eta$, where $d_\mathrm{e}^2 = m_\mathrm{e}/(\mu_0 e^2 n_0)$ is the square of the electron skin depth. Accordingly, the reduced form of the general two-fluid tearing dispersion relation (94) becomes

$$\frac{\hat{\gamma}^{5/4}}{(1+\mu\hat{\alpha}^2\hat{\gamma})^{3/4}}\, D\left(\frac{\hat{\gamma}^{1/2}\hat{\alpha}}{(1+\mu\hat{\alpha}^2\hat{\gamma})^{1/2}}, \frac{C^2\hat{\gamma}^{3/2}}{\pi^2\hat{\beta}(1+\mu\hat{\alpha}^2\hat{\gamma})^{1/2}}\right) = C. \tag{A.2}$$

The range $\epsilon_\eta \ll \epsilon_\gamma \mu\alpha^2$ or, in terms of the collision frequency, $\nu \equiv e^2 n_0 \eta/m_\mathrm{e} \ll \gamma$, corresponds to the collisionless tearing mode, where the electron inertia dominates over the resistive diffusivity as the leading effect to break the magnetic frozen-in law. In the collisionless limit, the first argument of $D(\sigma, \tau)$ in equation (A.2) becomes large ($\sigma = \mu^{-1/2} \gg 1$) so the

relevant parametric regions are likely to be the strong-Hall regimes, which leaves out PR2 and the high-beta subdomain of PR1. In dimensionless reduced form, the growth rate of the collisionless tearing mode, $\hat{\gamma}(\hat{\alpha}, \hat{\beta}, \mu)$, is

$$\begin{aligned}
&\hat{\gamma} = \mu^{3/2}\hat{\alpha}^3 && \text{for} \quad \hat{\beta} \ll \mu^2\hat{\alpha}^2 && \text{(PR1)},\\
&\hat{\gamma} = \mu^{3/2}\hat{\alpha}^3 f_6^{-2}\left(\frac{\pi^2\hat{\alpha}\hat{\beta}}{C^2\mu^{1/2}\hat{\gamma}}\right) && \text{for} \quad \hat{\beta} = O(\mu^2\hat{\alpha}^2) && \text{(PR6)},\\
&\hat{\gamma} = \mu^{1/2}\hat{\alpha}^2\hat{\beta}^{1/2} && \text{for} \quad \mu^2\hat{\alpha}^2 \ll \hat{\beta} \ll \mu\hat{\alpha}^2 && \text{(PR5)},\\
&\hat{\gamma} = \mu\hat{\alpha}^3 f_4^{-2}\left(\frac{C^2\hat{\gamma}}{\pi^2\hat{\alpha}\hat{\beta}}\right) && \text{for} \quad \hat{\beta} = O(\mu\hat{\alpha}^2) && \text{(PR4)},\\
&\hat{\gamma} = \mu\hat{\alpha}^3 && \text{for} \quad \mu\hat{\alpha}^2 \ll \hat{\beta} && \text{(PR3)}.
\end{aligned} \tag{A.3}$$

The expression for PR3 coincides with the collisionless electron-MHD form derived in [3, 4].

Figure 7 plots $\hat{\gamma}(\hat{\alpha}, \hat{\beta})$ covering both resistive and collisionless regimes, for a deuterium plasma. For the sake of illustration, simple patchings at lines representing, on the one hand, the intermediate regions PR2, PR4 and PR6, and on the other hand, the resistive-to-collisionless transition region (i.e. $\mu\hat{\alpha}^2\hat{\gamma} \sim 1$), have been used when generating the plot.

Depending on the relative values of $\epsilon_\eta$ and $m_e/m_i$, the sonic range of the growth rate is reached within the resistive or the collisionless limit. In the collisionless limit (and taking $kL_B \sim k^{-1}\Delta' \sim 1$), the subsonic and purely growing range of the tearing mode correspond to $\beta \gg \mu^2\alpha^6$ in PR3, $1 \gg \mu\alpha^4$ in PR4 to PR6 and $\beta \gg \mu^3\alpha^6$ in PR1. Figure 8 shows the sonic boundary for three different plasmas resistivities. If $\epsilon_\eta \ll \mu^{5/4}$ (a realistic case since $\mu^{5/4} \sim 3 \times 10^{-5}$ for deuterium), the tearing mode becomes sonic within the very-low-beta resistive subdomain of PR1 for $kd_e \ll \epsilon_\eta^{1/5}$ and within collisionless subregions for $kd_e \gg \epsilon_\eta^{1/5}$.

## References


[1] Furth H, Killeen J and Rosenbluth M 1963 *Phys. Fluids* **6** 459
[2] Mirnov V V, Hegna C C and Prager S C 2004 *Phys. Plasmas* **11** 4468
[3] Bulanov S, Pegoraro F and Sakharov A 1992 *Phys. Fluids* B **4** 2499
[4] Fruchtman A and Strauss H 1993 *Phys. Fluids* B **5** 1408
[5] Drake J and Lee Y 1977 *Phys. Fluids* **20** 1341
[6] Pegoraro F and Schep T 1986 *Plasma Phys. Control. Fusion* **28** 647
[7] Kuvshinov B 1994 *Plasma Phys. Control. Fusion* **36** 867
[8] Hazeltine R and Meiss J 1992 *Plasma Confinement* (Redwood, CA: Addison-Wesley)
[9] Abramowitz M and Stegun I 1965 *Handbook of Mathematical Functions* (New York: Dover)
[10] Jardin S C *et al* 2008 Two-fluid and resistive nonlinear simulations of tokamak equilibrium, stability and reconnection *IAEA-CN-165: 22nd IAEA Fusion Energy Conf. (Geneva, Switzerland, October 2008)* (Vienna: IAEA) TH/P9-29 http://www-pub.iaea.org/napc/physics/FEC/FEC2008/html/index.htm